Acta Crystallographica Section C
Crystal Structure Communications
ISSN 0108-2701

Asymmetric ruthenium-catalysed [2+2] cycloadditions between bicyclic alkenes and chiral aryl-substituted acetylenic acyl camphorsultam alkynes

Jordan D. Goodreid,[a] Michael C. Jennings[b]* and William Tam[a]

[a]Department of Chemistry, University of Guelph, 50 Stone Road East, Guelph, Ontario, Canada N1G 2W1, and [b]185 Chelsea Avenue, London, Ontario, Canada N6J 3J5
Correspondence e-mail: mjennings@teksavvy.com

Received 14 September 2009
Accepted 29 October 2009
Online 21 November 2009

The regio- and absolute stereochemistry of (7*S*)-*N*-[4-(3-thienyl)tricyclo[4.2.1.0^{2,5}]non-3-en-3-ylcarbonyl]-2,10-camphorsultam tetrahydrofuran hemisolvate, $C_{24}H_{29}NO_3S_2{\cdot}0.5C_4H_8O$, and (7*S*)-*N*-[4-(4-tolyl)tricyclo[4.2.1.0^{2,5}]non-3-en-3-ylcarbonyl]-2,10-camphorsultam, $C_{27}H_{33}NO_3S$, have been established. One contains a half-occupancy tetrahydrofuran solvent molecule located on a twofold axis and the other contains two crystallographically unique molecules which are nearly identical. The extended structures of both complexes can be explained *via* weak C—H$\cdots$O interactions, which link the molecules together into two-dimensional sheets in the *ab* plane for the thienyl complex and ultimately into a three-dimensional structure for the tolyl derivative. The stereochemistry of both structures confirms that [2+2] cycloadditions of bicyclic alkenes and alkynes catalysed by ruthenium are exclusively *exo*.

Comment

Recently, the metal-catalysed [2+2] cycloaddition reaction between bicyclic alkenes and alkynes has been utilized by several research groups as a means to generate cyclobutene rings. In terms of an asymmetric version of this process, both a chiral rhodium catalyst (Shibata *et al.*, 2006) and a ruthenium-catalysed reaction (Villeneuve & Tam, 2004) involving a chiral precursor have produced chiral [2+2] cyclobutene products. The ruthenium-catalysed [2+2] cycloaddition between norbornene and a phenylacetyleneacyl camphorsultam (chiral) yielded two diastereomers in a 131:1 ratio. The absolute stereochemistry of the major diastereomer (V) was established by single-crystal X-ray diffraction (Lough *et al.*, 2004).

As an extension of this study, the Tam group is investigating the selectivity effect of different organic groups attached at the acetylenic position (see scheme). In this paper, we present the results of ruthenium-catalysed [2+2] cycloadditions of norbornene, (I), with 3-thiophenylacetyleneacylcamphorsultam, (III), and 4-tolylacetyleneacylcamphorsultam, (IV). This yielded the expected complexes (7*S*)-*N*-[4-(3-thienyl)tricyclo[4.2.1.0^{2,5}]non-3-en-3-ylcarbonyl]-2,10-camphorsultam tetrahydrofuran hemisolvate, (VI), and (7*S*)-*N*-[4-(4-tolyl)-tricyclo[4.2.1.0^{2,5}]non-3-en-3-ylcarbonyl]-2,10-camphorsultam, (VII). Two diastereomers of (VI) were obtained in a 20:1 ratio,

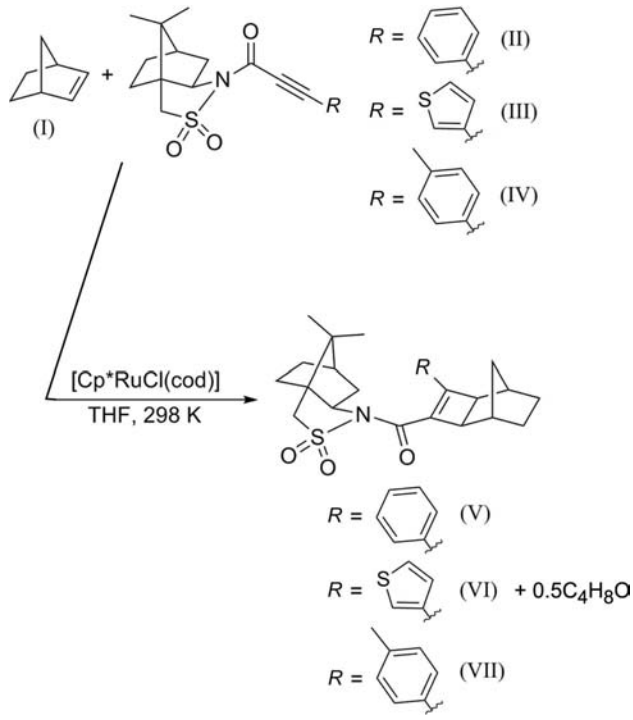

whereas the major stereoisomer of (VII) was obtained in a 104:1 ratio over the minor isomer. The absolute stereochemistry of the major isomers of (VI) and (VII) was estab-

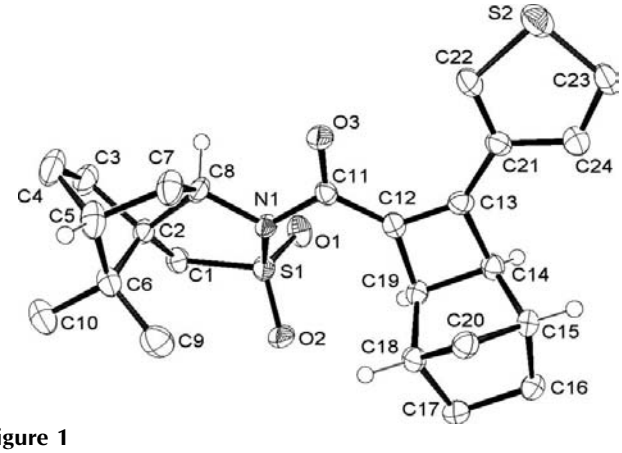

Figure 1
A view of the structure of (VI), showing the crystallographic labelling scheme. Displacement ellipsoids are drawn at the 50% probablility level. For the sake of clarity, nonchiral H atoms have been omitted, as has the partial-occupancy THF molecule of solvation.

 doi:10.1107/S0108270109045284

lished by the single-crystal X-ray diffraction analysis described here.

A view of (VI) is shown in Fig. 1. Elucidation of the X-ray structure establishes the absolute configuration of the following atoms in Fig. 1: C2-*S*, C5-*R*, C8-*R*, C14-*S*, C15-*R*, C18-*S* and C19-*R*. This is the same configuration as that observed for the phenyl derivative (V) (Lough *et al.*, 2004). There is a tetrahydrofuran (THF) solvent molecule occluded in the structure. It was modelled at half-occupancy, as it is located about ($\frac{1}{2}$, $\frac{1}{2}$, 0), which lies on a twofold axis along the [110] vector. The THF molecule was refined giving reasonable displacement parameters; the O atom of this molecule is involved in the weak interactions discussed below.

There are two chemically identical molecules of (VII) in the asymmetric unit. They are very similar structurally, with an r.m.s. fit of 0.207 Å (*PLATON*; Spek, 2009). As expected, both have the same configuration as that observed for (VI). The absolute configuration, as determined by anomalous dispersion, is as follows: C2-*S*, C5-*R*, C8-*R*, C14-*S*, C15-*R*, C18-*S* and C19-*R* for one molecule, and C32-*S*, C35-*R*, C38-*R*, C44-*S*, C45-*R*, C48-*S* and C49-*R* for the second. The structure of one of the molecules of (VII) is shown in Fig. 2. The crystallographic difference in the two molecules is primarily attributed to their spatially different orientations with respect to one another (see below). The geometric data for both (VI) and (VII) are in the normal ranges.

Weak C—H···O interactions in (VI) (see Table 1 for geometric parameters and symmetry codes) link the molecules. Perhaps the simplest method to describe the packing is by using two 'classical model' graph-set descriptors (Bernstein *et al.*, 1995). Firstly, a 'chain of rings' is formed through two weak interactions (C8—H8*A*···O2^{i} and C1—H1*B*···O3^{ii}) that link molecules together into ribbons along the *a* axis {motif $C_2^2(10)[R_2^2(9)]$; Fig. 3}. Secondly, adjacent ribbons are linked together *via* reciprocating C14—H14*A*···O1^{iii} interactions. It should be noted that these are the 'weakest' of the weak interactions mentioned herein. There are two further layers in the extension along the *c* axis, each of which is rotated by 120° with respect to the previous layer. The THF solvent molecule was refined at half-occupancy, as it is located on a rotational axis; the O atom links to one of the layers *via* another weak interaction (C1—H1*A*···O31).

As with (VI), it is the weak C—H···O interactions that control the geometry observed in the crystal structure of (VII) (Table 2). The nine weak interactions lead to a very extensive set of hydrogen-bonding motifs so only the key graph-set descriptors are noted here. The asymmetric unit contains two molecules, which couple together *via* two weak interactions (C3—H3*B*···O31 and C31—H31*B*···O3) to form an 11-membered ring, and, adjacent to this, a nine-membered ring is formed *via* C38—H38*A*···O1^{i} and C1—H1*B*···O33^{ii} interactions. This quaternary graph set, somewhat similar to that in (VI), has the motifs $C_2^2(10)[R_2^2(11)R_2^2(9)]$: a 'chain of rings' yielding ribbons along the *a* axis (Fig. 4). These *a*-axis ribbons are connected up and down the *c* axis according to the binary

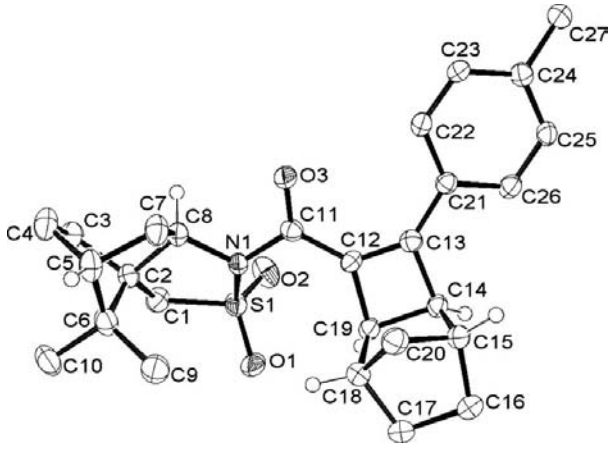

Figure 2
The molecular structure of one of the molecules of (VII), showing the atom-labelling scheme and with displacement ellipsoids drawn at the 50% probability level. For the sake of clarity, the nonchiral H atoms have been omitted.

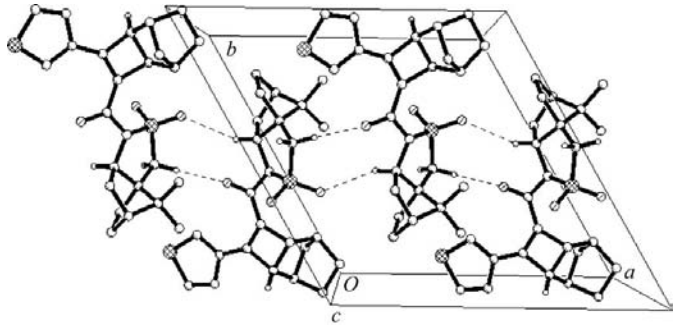

Figure 3
The packing of (VI), showing the primary chain-forming C—H···O interactions as dashed lines. All H atoms, except those attached to atoms involved in weak interactions, have been omitted for clarity. The view is approximately down the *c* axis, showing the ribbons along the *a* axis.

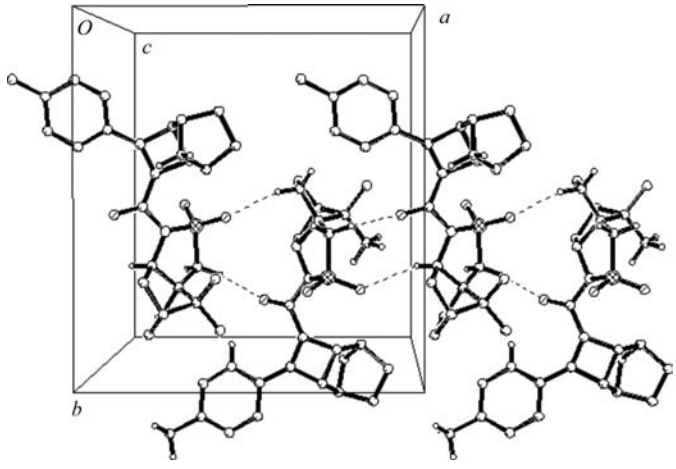

Figure 4
The packing of (VII), showing the primary chain-forming C—H···O interactions as dashed lines. All H atoms, except those involved in the displayed weak interactions, have been omitted for clarity. The view is approximately down the *c* axis, showing the formation of a chain along the *a* axis.

graph-set descriptor $C_2^2(12)$ *via* C50—H50*A*···O2^{iii} and C9—H9*A*···O3^{iv} interactions, thus forming parallel ribbons in the [010] plane. Finally, a full three-dimensional network is established *via* C27—H27*A*···O32^{v} and C9—H9*A*···O3^{iv} interactions, making $C_2^2(25)$ connections along the *b* axis. For completeness, the last two interactions in Table 2 can be described by motif *S*(7).

While there are no classical hydrogen-bonding networks in either of these structures, the weak interactions do seem to explain the observed geometry, which is understandable as even a weak hydrogen bond will be stronger than the van der Waals interactions. Unlike the previously published phenyl cycloadduct which shows partial π–π stacking between neighbouring phenyl rings (closest contact = 3.64 Å) through secondary orbital overlap interactions (Lough *et al.*, 2004), no such π-stacking interactions between either thiophenyl rings or tolyl rings are observed in these crystal structures.

In the case of the [2+2] cycloaddition, these crystal structures have unambiguously identified which are the major diastereomers formed in the asymmetric cycloaddition. The previous phenyl derivative combined with both the thiophenyl and the tolyl derivatives herein reaffirm that [2+2] cycloadditions of bicyclic alkenes and alkynes catalysed by ruthenium are exclusively *exo* with respect to their stereochemistry.

Experimental

Preparation of compound (VI) was achieved by addition of norbornene (72.0 mg, 765 mmol), (I), and chiral alkyne (III) (52.2 mg, 0.149 mmol) to Cp*Ru(cod)Cl (Cp* is pentamethylcyclopentadienyl and cod is 1,5-cyclooctadiene; 7.6 mg, 0.020 mmol) in THF (0.6 ml). The mixture was stirred for 18 h at 298 K, and subsequent column chromatography of the crude reaction mixture provided a 98% yield of the two diastereomeric cycloadducts in a 20:1 ratio. Evaporative recrystallization of the column-purified product in THF provided the major diastereomer (VI), giving colourless crystals suitable for X-ray analysis. Similarly, compound (VII) was prepared by addition of norbornene (83.0 mg, 0.881 mmol), (I), and chiral alkyne (IV) (63.2 mg, 0.177 mmol) to Cp*Ru(cod)Cl (7.1 mg, 0.018 mmol) in THF (0.5 ml). The mixture was stirred for 17 h at 298 K, and subsequent column chromatography of the crude reaction mixture provided a 79% yield of the two diastereomeric cycloadducts in a 104:1 ratio. Evaporative recrystallization of the column-purified product in THF provided major diastereomer (VII), giving colourless crystals suitable for X-ray analysis. Both diastereomeric ratios were back-calculated from the corresponding *ee* values obtained through cleavage of the chiral auxiliary under reductive conditions ($LiAlH_4$, $AlCl_3$), giving an enantiomeric mixture of cycloadduct alcohols that can be resolved using a Chiralcel OJ-H high-performance liquid chromatography column.

Compound (VI)

Crystal data

$C_{24}H_{29}NO_3S_2{\cdot}0.5C_4H_8O$
M_r = 479.65
Trigonal, $P3_221$
a = 12.0797 (17) Å
c = 28.326 (6) Å
V = 3579.5 (10) Å^3
Z = 6
Mo $K\alpha$ radiation
μ = 0.25 mm^{-1}
T = 150 K
0.35 × 0.22 × 0.15 mm

Table 1
Hydrogen-bond geometry (Å, °) for (VI).

D—H···*A*	*D*—H	H···*A*	*D*···*A*	*D*—H···*A*
C8—H8*A*···O2^{i}	1.00	2.59	3.516 (3)	154
C1—H1*B*···O3^{ii}	0.99	2.45	3.422 (3)	168
C14—H14*A*···O1^{iii}	1.00	2.66	3.500 (3)	141
C1—H1*A*···O31	0.99	2.36	3.235 (14)	147

Symmetry codes: (i) $x-y, -y+1, -z+\frac{1}{3}$; (ii) $x-y+1, -y+1, -z+\frac{1}{3}$; (iii) $x-y+1, -y+2, -z+\frac{1}{3}$.

Table 2
Hydrogen-bond geometry (Å, °) for (VII).

D—H···*A*	*D*—H	H···*A*	*D*···*A*	*D*—H···*A*
C3—H3*B*···O31	0.99	2.58	3.539 (3)	163
C31—H31*B*···O3	0.99	2.45	3.356 (2)	152
C38—H38*A*···O1^{i}	1.00	2.54	3.412 (2)	146
C1—H1*B*···O33^{ii}	0.99	2.37	3.332 (3)	164
C50—H50*A*···O2^{iii}	0.99	2.53	3.446 (2)	153
C9—H9*A*···O3^{iv}	0.98	2.59	3.570 (3)	174
C27—H27*A*···O32^{v}	0.98	2.43	3.404 (3)	174
C22—H22*A*···O3	0.95	2.31	3.115 (3)	142
C52—H52*A*···O33	0.95	2.33	3.129 (3)	141

Symmetry codes: (i) $x-1, y, z$; (ii) $x+1, y, z$; (iii) $-x+1, y-\frac{1}{2}, -z+\frac{3}{2}$; (iv) $x+\frac{1}{2}, -y+\frac{3}{2}, -z+2$; (v) $x, y+1, z$.

Data collection

Nonius KappaCCD diffractometer
Absorption correction: multi-scan (*DENZO–SMN*; Otwinowski & Minor, 1997)
T_{min} = 0.916, T_{max} = 0.963
8354 measured reflections
4207 independent reflections
3310 reflections with $I > 2\sigma(I)$
R_{int} = 0.041

Refinement

$R[F^2 > 2\sigma(F^2)]$ = 0.038
$wR(F^2)$ = 0.084
S = 1.01
4207 reflections
318 parameters
4 restraints
H-atom parameters constrained
$\Delta\rho_{max}$ = 0.19 e Å^{-3}
$\Delta\rho_{min}$ = −0.31 e Å^{-3}
Absolute structure: Flack (1983), 1788 Friedel pairs
Flack parameter: −0.03 (7)

Compound (VII)

Crystal data

$C_{27}H_{33}NO_3S$
M_r = 451.60
Orthorhombic, $P2_12_12_1$
a = 11.687 (2) Å
b = 12.849 (3) Å
c = 31.547 (6) Å
V = 4737.2 (16) Å^3
Z = 8
Mo $K\alpha$ radiation
μ = 0.17 mm^{-1}
T = 150 K
0.40 × 0.35 × 0.17 mm

Data collection

Nonius KappaCCD diffractometer
Absorption correction: multi-scan (*DENZO–SMN*; Otwinowski & Minor, 1997)
T_{min} = 0.937, T_{max} = 0.972
44242 measured reflections
9673 independent reflections
7676 reflections with $I > 2\sigma(I)$
R_{int} = 0.068

Refinement

$R[F^2 > 2\sigma(F^2)]$ = 0.041
$wR(F^2)$ = 0.096
S = 1.03
9673 reflections
583 parameters
H-atom parameters constrained
$\Delta\rho_{max}$ = 0.19 e Å^{-3}
$\Delta\rho_{min}$ = −0.31 e Å^{-3}
Absolute structure: Flack (1983), 4291 Friedel pairs
Flack parameter: −0.02 (5)

Both the O—C bonds and the C—C bonds of the disordered solvent (THF) were restrained, respectively, to be identical. H atoms were positioned geometrically and refined using a riding model, with C—H distances of 0.98 (CH_3), 0.99 (CH_2), 1.00 (CH) or 0.95 Å (aromatic CH). U_{iso}(H) values were set at 1.2 times U_{eq}(C) for all except the methyl H atoms, for which U_{iso}(H) = 1.5U_{eq}(C).

For both compounds, data collection: *COLLECT* (Nonius, 1997); cell refinement: *DENZO–SMN* (Otwinowski & Minor, 1997); data reduction: *DENZO–SMN*; program(s) used to solve structure: *SHELXS97* (Sheldrick, 2008); program(s) used to refine structure: *SHELXL97* (Sheldrick, 2008); molecular graphics: *SHELXTL/PC* (Sheldrick, 2008); software used to prepare material for publication: *SHELXTL/PC*.

The authors acknowledge NSERC Canada, the University of Western Ontario and the University of Guelph for funding.

Supplementary data for this paper are available from the IUCr electronic archives (Reference: GA3134). Services for accessing these data are described at the back of the journal.

References

Bernstein, J., Davis, R. E., Shimoni, L. & Chang, N.-L. (1995). *Angew. Chem. Int. Ed.* **34**, 1555–1573.
Flack, H. D. (1983). *Acta Cryst.* A**39**, 876–881.
Lough, A. J., Villeneuve, K. & Tam, W. (2004). *Acta Cryst.* E**60**, o1566–o1567.
Nonius (1997). *KappaCCD Server Software*. Windows 3.11 Version. Nonius BV, Delft, The Netherlands.
Otwinowski, Z. & Minor, W. (1997). *Methods in Enzymology*, Vol. 276, *Macromolecular Crystallography*, Part A, edited by C. W. Carter Jr & R. M. Sweet, pp. 307–326. New York: Academic Press.
Sheldrick, G. M. (2008). *Acta Cryst.* A**64**, 112–122.
Shibata, T., Takami, K. & Kawashi, A. (2006). *Org. Lett.* **8**, 1343–1345.
Spek, A. L. (2009). *Acta Cryst.* D**65**, 148–155.
Villeneuve, K. & Tam, W. (2004). *Angew. Chem. Int. Ed.* **43**, 610–613.